

Temperature Knowledge and Model Correlation for the Soil Moisture Active and Passive (SMAP) Reflector Mesh

Rebecca Mikhaylov¹, Douglas Dawson², and Eug Kwack³
Jet Propulsion Laboratory, California Institute of Technology, Pasadena, California, 91109

NASA's Earth observing Soil Moisture Active & Passive (SMAP) Mission is scheduled to launch in November 2014 into a 685 km near-polar, sun synchronous orbit. SMAP will provide comprehensive global mapping measurements of soil moisture and freeze/thaw state in order to enhance understanding of the processes that link the water, energy, and carbon cycles. The primary objectives of SMAP are to improve worldwide weather and flood forecasting, enhance climate prediction, and refine drought and agriculture monitoring during its 3 year mission. The SMAP instrument architecture incorporates an L-band radar and an L-band radiometer which share a common feed horn and parabolic mesh reflector. The instrument rotates about the nadir axis at approximately 15 rpm, thereby providing a conically scanning wide swath antenna beam that is capable of achieving global coverage within 3 days. In order to make the necessary precise surface emission measurements from space, a temperature knowledge of 60°C for the mesh reflector is required. In order to show compliance, a thermal vacuum test was conducted using a portable solar simulator to illuminate a non flight, but flight-like test article through the quartz window of the vacuum chamber. The molybdenum wire of the antenna mesh is too fine to accommodate thermal sensors for direct temperature measurements. Instead, the mesh temperature was inferred from resistance measurements made during the test. The test article was rotated to five separate angles between 10° and 90° via chamber breaks to simulate the maximum expected on-orbit solar loading during the mission. The resistance measurements were converted to temperature via a resistance versus temperature calibration plot that was constructed from data collected in a separate calibration test. A simple thermal model of two different representations of the mesh (plate and torus) was created to correlate the mesh temperature predictions to within 60°C. The on-orbit mesh temperature will be predicted using the correlated analytical thermal model since direct measurements from in-situ flight thermal sensors are not possible.

Nomenclature

α	=	solar absorptivity
ε	=	emissivity
AM	=	ante meridiem
GN ₂	=	Gaseous Nitrogen
SMAP	=	Soil Moisture Active Passive Mission
TC	=	thermocouple
rpm	=	revolutions per minute

I. Introduction

A thermal vacuum test was conducted in a three-foot diameter vacuum chamber to verify compliance with the SMAP antenna mesh temperature knowledge requirement of 60°C. A portable solar simulator illuminated a non flight, but flight-like test article (9.75" x 9.75" antenna mesh with flight-like tensioning) through the quartz window of the vacuum chamber. The beam irradiance was a constant 1447 W/m² (at 22" from the window) during

¹ Instrument Thermal Engineer, Instrument Mechanical Thermal Subsystem, Mail Stop 125-123

² Radiometer System Engineer, Instrument Systems Engineering, Mail Stop 168-314

³ Lead Instrument Thermal Engineer, Instrument Mechanical Thermal Subsystem, Mail Stop 125-123

the entire test. The test article was rotated to five separate angles between 10° and 90° via chamber breaks to simulate the maximum expected on-orbit solar loading during the mission. Using both an analytical model (Ansys Maxwell 3-D) for current flow in the mesh and earlier characterization test data, the test article was designed to balance the goal of reduced measurement error (frame narrowed, mesh spacing between resistance measurements established) against the fragile mesh's capability to physically support the clamp and lug masses at the four measurement sites. A pre-test solar mapping of the portable solar simulator at three different locations (18, 22 and 26 inches from the window) was performed to verify beam uniformity/stability and to ensure proper test article illumination. The molybdenum wire of the antenna mesh is too fine to accommodate thermal sensors for direct temperature measurements. Instead, the mesh temperature was inferred from resistance measurements made during the test. The resistance measurements were converted to temperature via a resistance versus temperature calibration plot that was constructed from data collected in a separate calibration test previously performed in a 1-atm environmental chamber. The mesh temperatures varied from 129°C to 160°C according to test data over the investigated angular range, and these were subsequently adjusted (143°C to 173°C) using the Ansys Maxwell 3-D model because of the cooler frame temperatures. A simple thermal model of two different representations of the mesh (plate and torus) was created to correlate the mesh temperature predictions to within 60°C of the test results, and the torus thermal model fit the test data best. Although the mesh optical properties were not verified, the thermal model was correlated to within 60°C of the test data when the mesh α/ϵ was reduced from seven to four.

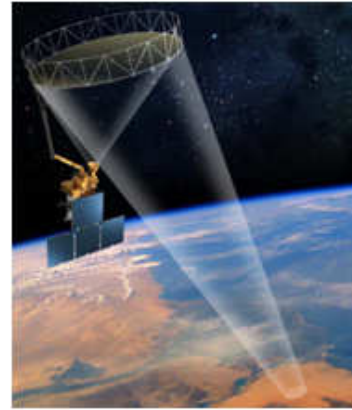


Figure 1. SMAP observatory with spinning 6m deployable mesh reflector antenna. The active radar and passive radiometer share a common L-band feed horn.

II. Test Objectives

Mesh temperature knowledge is critical to the radiometric performance so it is an allocated item in the instrument error budget. The on-orbit mesh temperature will be predicted using a correlated analytical thermal model since direct measurements from in-situ flight thermal sensors are not possible. The primary test objective is to use results from the mesh temperature knowledge test to verify requirement compliance which requires predicted antenna mesh temperature accuracy to within 60°C .

Due to the small wire thickness, a variety of options to measure the mesh temperature were originally considered and eliminated. One proposal to measure the wire resistance and correlate it to temperature was deemed viable. A concept development test was performed in November 2011 to verify the feasibility of this method; it was determined that measuring the mesh resistance could predict the temperature within a few degrees Celsius. The test described within utilizes the earlier concept for measuring the mesh temperature while simulating flight-expected conditions, including:

1. Flight-like mesh (material, thickness, tension)
2. Solar illumination (antenna angle)

The mesh temperature measurements from the test will then be used to correlate to a simple thermal model of two representations of the mesh (plate and torus) to verify if the temperature is predictable to within 60°C . The best-fit representation of the mesh thermal model will then be substituted for the mesh in the SMAP instrument-level thermal model.

III. Requirements

Two requirements are the basis of this test:

Knowledge: The change in the on-orbit physical temperature of the antenna reflector mesh from any one time when the observatory is not in eclipse to any other time when the observatory is not in eclipse shall be predicted to within 60°C .

Temperature Limits: The allowable flight temperatures of the reflector mesh shall not exceed -100°C to 260°C during operating conditions or -100°C to 280°C during non-operating conditions.

The knowledge requirement applies to the non-eclipse ante meridiem (AM) portion of the science orbit, which corresponds to a predicted mesh temperature range of approximately 0°C to 220°C (Figure 1) using a thin-plate mesh model. The results of this test will be used to verify the 60°C prediction capability of the thermal model.

IV. Test Article

The test article contains no flight hardware, but includes a flight-like sample of antenna mesh (1.2 mil gold-plated molybdenum wire with 20 openings per inch). The test article is composed of 9.75" x 9.75" antenna mesh with flight-like tensioning in a frame. Four copper clamps with wire lugs were installed (one near each corner of the frame) to measure both diagonal resistances through the mesh. Vacuum-deposited gold on Kapton tape was applied on the exterior frame surface that would be illuminated in the chamber to minimize the temperature difference between the tensioned mesh and the mesh adhered in the frame (Figure 2).



Figure 2. Mesh Temperature Knowledge test article.

An area of concern was the temperature knowledge error due to the mesh bonded under the frame whose temperature would be different from the center of the mesh. Using both MatLab and an Ansys Maxwell 3-D current model of the original test article configuration, the current flow through the mesh with 1 inch thick frame and clamps positioned 1.325 inches from the frame outer corner is shown in Figure 3. A predicted 27.8 percent of current goes through the mesh that is bonded between the two frame pieces (Table 1). As the clamps were moved diagonally inward on the mesh and further from the frame corners, the current flow underneath the frame decreased.

Two options were utilized to minimize the effects of the temperature difference between the mesh and the frame based on the current model predictions: the frame sides were thinned down from 1 inch to 0.25 inch; and, the copper clamps were installed at various positions from the frame corner. Table 1 summarizes the trade study used to quantify the current loss under the frame.

Due to the thin wire mesh and weight of the clamps, the mesh would distort under the weight of the clamps as they were positioned closer together. Table 1 results were used to optimize the position of the clamps such that the frame would provide adequate support for the clamp weight and mesh tension as well as minimize

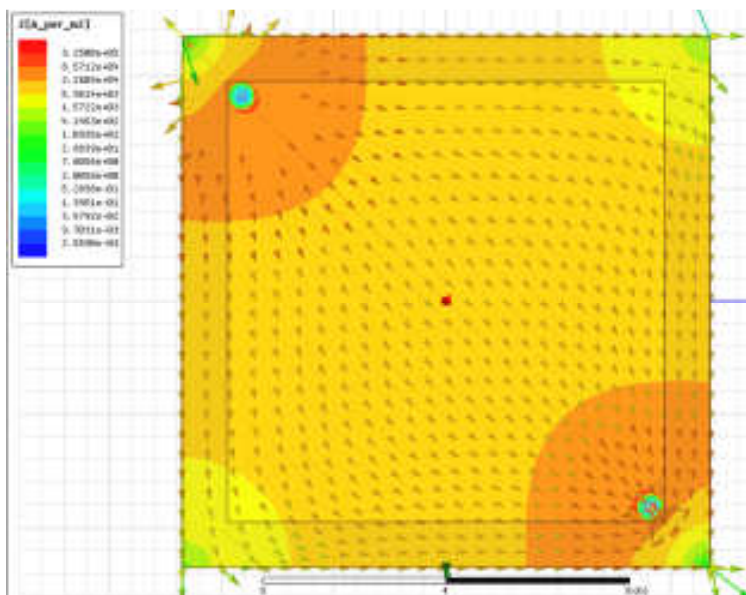


Figure 3. Current Loss through 1 in Frame with Copper Clamp Position of 1.325 in.

Table 1. Predicted Current Through Frame for Varying Frame Widths and Clamp Positions.

Clamp Location	1" Frame		0.25" Frame	
	% Current thru Mesh	Simulated Resistance, ohms	% Current thru Mesh	Simulated Resistance, ohms
0.7	--	--	89.8	1.79E-01
1.3	72.2	1.41E-01	92.0	--
2.0	77.6	1.13E-01	--	--
2.5	80.6	1.00E-01	--	--
3.0	83.0	8.87E-02	94.9	8.87E-02
3.5	85.1	7.76E-02	--	--
4.0	87.0	6.81E-02	--	--
4.5	88.8	5.77E-02	--	--
5.0	90.7	4.53E-02	--	--

the amount of current through the mesh under the frame.

The frame sides were thinned down from 1 inch to 0.25 inch; and, the copper clamps were installed at 1.325 inches from the frame corner, resulting in a predicted current through the mesh under the frame of less than 10%.

V. Test Facility and Set Up

The test was performed in a three-foot diameter vacuum chamber with a quartz window. The Spectrolab X-25 Solar Simulator beam is capable of producing up to 2.5 times the solar constant at 1 AU and includes a filter that produces a square illumination of approximately 9" x 9" at the 17.75" Quartz window cover location (Figure 4). The portable solar simulator was used to produce the equivalent of nearly one solar constant (1447 W/m² versus 1420 W/m²) incident upon the test article while the chamber was held at room temperature and under vacuum (<10⁻⁵ Torr). The chamber shroud was flooded with Gaseous Nitrogen (GN₂) to maintain room temperature within the chamber. The test was repeated at various test article angles of attack as expected on-orbit: 10°, 15°, 30°, 45°, and 90°. The angles of attack correspond to reflector mesh angles relative to the sun. Shadowing effects of the frame on the mesh are dominant for angles of attack 10° or less. Chamber breaks occurred to change the articulation of the test article.

The test article was attached to the chamber rail using fixed length wires with the center of the mesh at 22 inches into the chamber (Figures 5 and 6). An inclinometer was used to verify the angle of attack. Two calibration targets were positioned within 0.5 inch from the right and left sides of the frame at a depth of 22 inches from the chamber door.

VI. Instrumentation

In addition to facility instrumentation of the chamber, twelve Type E thermocouples were installed on the frame, calibration targets, Quartz window, and chamber door. The thermal data acquisitions system recorded and output the thermocouple temperature measurements at 60 second intervals.

A pair of resistance measurements were made by measuring changes in voltage for each angle of attack. The same unit was used for the Resistance-Temperature calibration test.

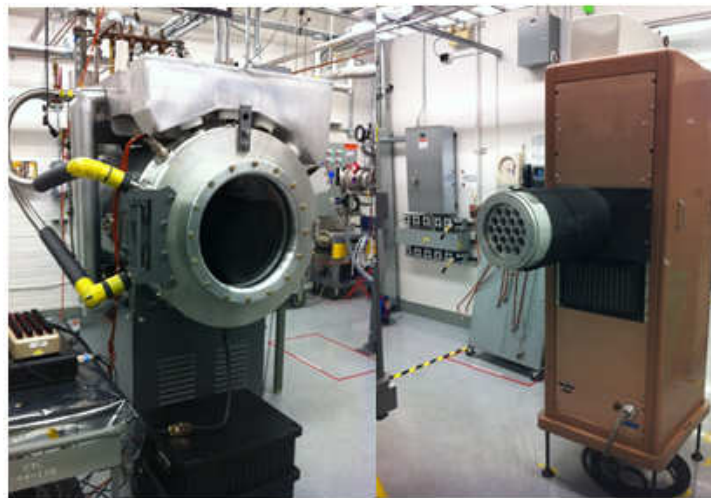


Figure 4. Three-foot vacuum chamber with Quartz window and Solar Simulator.

VII. Test Results and Discussion

Two pre-tests were performed prior to the main mesh test where the mesh temperatures (resistances) were measured with various angles of attack of the sun. The first pre-test was the Resistance-Temperature Calibration Test. The other pre-test was the Solar Beam Survey at 18, 22 and 26 inches.

The resistances of the mesh were measured at different angles of attack between 10° and 90° . It took approximately one hour to reach vacuum ($<10^{-5}$ Torr) after changing angles of attack. After vacuum was achieved, the solar simulator was turned on to 99 Amp. Results from the mapping test showed that 99 Amp provides near one solar constant at chamber depth of 22 inches. The mesh temperatures (resistance values) reach asymptotic values nearly instantaneously (within 1 minute) due to the tiny thermal capacitance of the mesh. The frame temperatures reach steady state very gradually and take more than 60 minutes (Figure 7). In Figure 7, Targets 1 through 8 are the frame thermocouple temperatures and Targets 9 and 10 are calibration target 1 and 2 temperatures, respectively. Figures 8 and 9 are images of the test at angles of attack of 90° and 45° , respectively.

It was observed that the resistance values at room temperature varied after a configuration change. However, the resistance value increases during the test with a larger angle of attack as expected (Table 2) except from 30° to 45° angle of attack. The test was repeated at 30° angle of attack, and the results were very close to each other. As the measured values are compared with the predicted values, the measured value at 45° angle of attack seems too low. However, the measurement at 45° angle of attack was not repeated due to time constraints.

The frame temperatures for all angles of attack are shown in Table 3. Frame temperature decreases with decreasing angle of attack except for selective thermocouples depending on their location. When the angle of attack decreased from 90° , the copper tabs of these thermocouples were exposed to the solar beam. The temperature difference between the front and back of the frame is as large as 8.2°C at the largest angle of attack (90°) but reduced to as small as 2.7°C when the angle of attack is at the minimum (10°). Selective thermocouples were used to estimate frame averaged temperatures.

An Ansys Maxwell 3-D model consisting of a conducting plate as a model for the mesh and perfectly conductive wires driving current into the model at locations similar to the actual physical location of the copper contacts on the test article was created. Based on the thermocouple readings of the test article at different incident angles listed in Table 5, a fixed temperature was assigned to the mesh material under the frame while the unencumbered mesh was forced from 20°C to 260°C . The total resistance between the contacts was generated.

Thermal Desktop models of a flat plate and torus were developed. The flat plate and torus temperatures were calculated using assumed optical properties and solar intensities. The results shown in Figure 10 use the measured mesh temperatures with

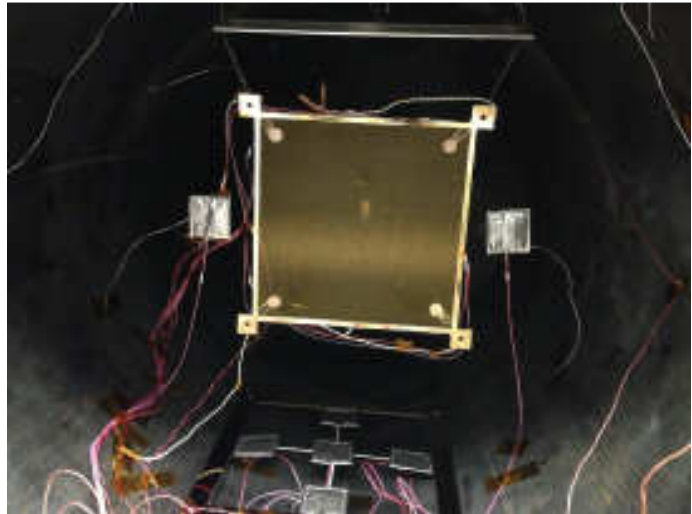


Figure 5. Temperature Knowledge Test Article Set-up at 90° .

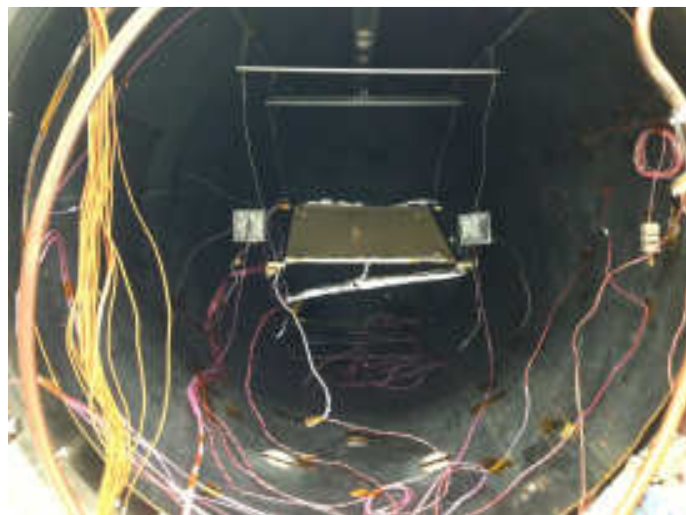


Figure 6. Temperature Knowledge Test Article Set-up at 15° .

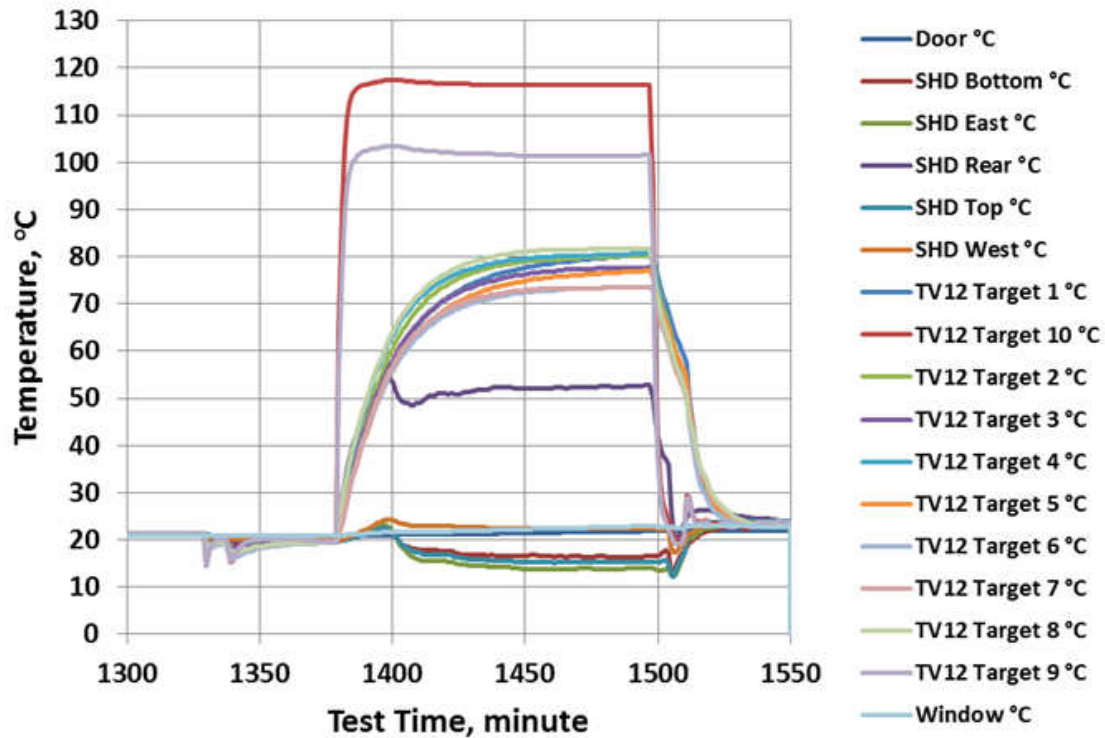


Figure 7. Current Loss through 1 in Frame with Copper Clamp Position of 1.325 in.

frame temperature corrections and show that the torus model can be used more accurately to predict the mesh temperature. The torus model predicted values demonstrate similar behavior with the measured values but the predicted values are larger than the measured by 46°C to 59°C (Table 4).

The optical properties of the mesh are not easily measured since the mesh is very thin (1.2 mil thick). The ratio of the solar absorptivity to the IR emissivity of the mesh is unverified. Using the torus thermal model with different values of the α/ϵ ratio is shown in Table 4. Assuming $\alpha/\epsilon = 4$, the difference between the measured and torus thermal model can be less than 6°C, which is much smaller than the 60°C knowledge requirement.

VIII. Conclusion

An electrical resistance measurement can be a good indirect method to measure temperature of a thin wire mesh. The woven mesh used in the SMAP reflector can be modeled using simple torus geometry. The measured mesh temperatures were well correlated (within 10°C) by a simple torus model with optical property ratio of $\alpha/\epsilon = 4$, which is lower than $\alpha/\epsilon = 7$ originally assumed and within the 60°C knowledge requirement.

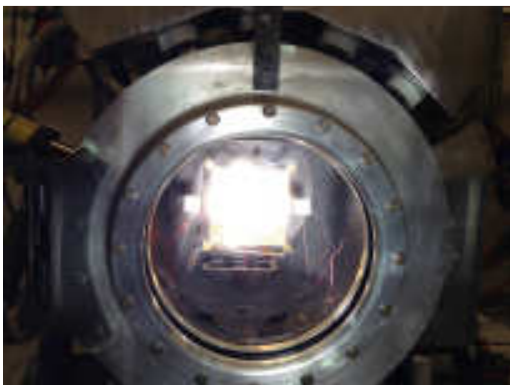


Figure 8. Temperature Knowledge Test at 90°.

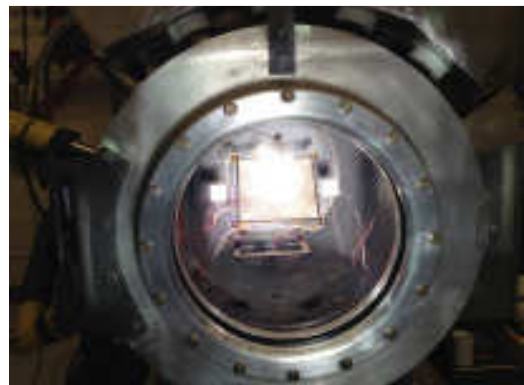


Figure 9. Temperature Knowledge Test at 45°.

Table 2. Predicted Current Through Frame for Varying Frame Widths and Clamp Positions.

Angle of Attack [°]	Resistance (Ω)			Temperature ($^{\circ}\text{C}$)			T^*_{avg} ($^{\circ}\text{C}$)
	dia1	dia2	avg	dia1	dia2	avg	
90	0.502	0.497	0.500	160.7	159.3	160.0	173
45	0.463	0.461	0.462	150.1	149.5	149.8	160
30	0.482	0.476	0.479	152.2	150.6	151.4	161
15	0.420	0.417	0.419	137.3	136.5	136.9	149
10	0.399	0.391	0.395	129.8	127.7	128.8	143

* Includes Frame Temperature Correction

Table 3. Frame Temperatures with Various Angles of Attack.

TC	Angle of Attack, ($^{\circ}$)				
	90	45	30	15	10
Frame 1	80.0	100.7	103.3	97.6	92.4
Frame 2	80.1	100.4	104.0	100.7	97.5
Frame 3	77.6	71.2	49.1	54.8	43.5
Frame 4	80.5	72.7	65.9	55.1	54.1
Frame 5	76.7	73.3	68.1	55.9	53.7
Frame 6	73.4	82.1	82.1	86.6	75.9
Frame 7	73.4	67.7	61.7	56.8	52.8
Frame 8	81.6	74.3	67.5	60.5	55.5

Table 4. Torus Thermal Model and Mesh Temperature Correlation.

T_{avg} ($^{\circ}\text{C}$)	$\alpha/\varepsilon = 7$		$\alpha/\varepsilon = 5$		$\alpha/\varepsilon = 4$	
	Torus, $^{\circ}\text{C}$	ΔT , $^{\circ}\text{C}$	Torus, $^{\circ}\text{C}$	ΔT , $^{\circ}\text{C}$	Torus, $^{\circ}\text{C}$	ΔT , $^{\circ}\text{C}$
173.0	232.1	59	199.7	27	176.9	4
160.0	218.6	59	186.3	26	165.6	6
161.0	207.0	46	176.1	15	157.7	-3
149.0	197.7	49	167.3	18	147.9	-1
143.0	194.4	51	164.3	21	146.0	3

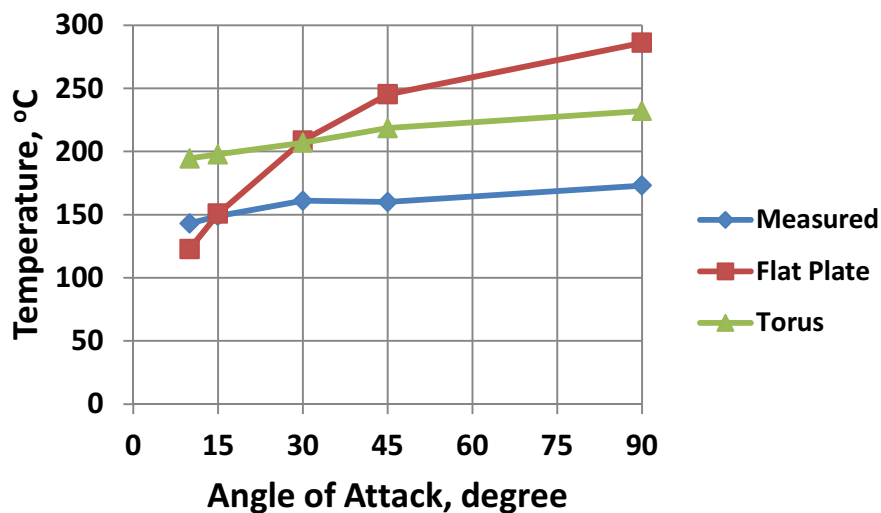


Figure 10. Frame Temperature Effects with various Angles of Attack.

Acknowledgments

The authors would like to acknowledge the following people for their contribution to the successful completion of this test: Gerald Gaughen for assembly of the test article; Dominic Aldi for calibration test facility and support; Bernard Rax for loan of a Source Meter; Rich Frisbee for assembly of the test article and support, and installation inside the chamber; Sandro Torres for instrumentation; Simeon Young, Mike Sachse, and Anton Ovcharenko for test support; Paula Brown for the antenna mesh sample; and, Gary Kinsella for technical review of the test and report.

The research was carried out at the Jet Propulsion Laboratory, California Institute of Technology, under a contract with the National Aeronautics and Space Administration.

© 2014 California Institute of Technology. Government sponsorship acknowledged.

References

- [1] Entekhabi, D., Njoku, E.G., O'Neill, P.E., Kellogg, K., Crow, W., Edelstein, W., et. al., "The Soil Moisture Active Passive (SMAP) Mission," *Proceedings of the IEEE*, Vol. 98, No. 5, IEEE, Boston, MA, 2010, pp. 704-716.
- [2] Entekhabi, D., Njoku, E., O'Neill, P., Spencer, M., Jackson, T., Entin, J., Im, E., and Kellogg, K., "The Soil Moisture Active/Passive Mission (SMAP)," *Geoscience and Remote Sensing Symposium, 2008. IGARSS 2008. IEEE International*, Vol. 3, IEEE, 2008, pp. III - 1-III - 4.
- [3] Entekhabi, D., Jackson, T.J., Njoku, E., O'Neill, P., Entin, J., "Soil Moisture Active/Passive (SMAP) Mission Concept," *Atmospheric and Environmental Remote Sensing Data Processing and Utilization IV: Readiness for GEOSS II*, SPIE, Vol. 7085, 2008, pp. 70850H-1-70850H-6.
- [4] Kim, S., van Zyl, J., McDonald, K., and Njoku, E., "Monitoring surface soil moisture and freeze-thaw state with the high-resolution radar of the Soil Moisture Active/Passive (SMAP) mission," *Radar Conference, 2010 IEEE*, 2010, pp. 735-739.
- [5] O'Neill, P., Entekhabi, D., Njoku, E., and Kellogg, K., "The NASA Soil Moisture Active Passive (SMAP) Mission: Overview," *Geoscience and Remote Sensing Symposium (IGARSS), 2010 IEEE International*, IEEE, 2010, pp. 3236-3239.